SUPPLEMENTAL DATA

SUPPLEMENTAL EXPERIMENTAL PROCEDURES

Measurement of Mitotic Index

Mitotic index, as determined by the abundance of phosphorylated histone H3, a marker for mitosis (Hans and Dimitrov, 2001), was estimated by immunofluorescence and immunoblotting (in Figure S2) as described previously (Chmielowiec et al., 2007; Kodani and Sutterlin, 2008).

Scratch-wound Assays

Scratch wound assays were carried out (in Figure 1A, B, S1B, 6F) as described previously (Ghosh et al., 2008). To quantify cell migration (expressed as % wound area covered), images were analyzed using Image J (NIH) software to calculate the difference between the wound area at 0 min and at the end of the migration assay divided by the area at 0 min x 100.

Growth Curves

Confluent monolayers of HeLa cells stably expressing siRNA-resistant GIV-wt or GIVF1685A (at levels ~3 fold above endogenous GIV) or GIVΔCT (at levels similar to those observed in poorly metastatic MCF7 cells) or empty vector were maintained in 10% FBS supplemented with penicillin, streptomycin and 500 µg G418. Control HeLa cells were maintained under identical conditions, except that G418 was excluded. Each cell line was seeded at a density of 2 x 10^4 cells/ well (6-well plate), cultured in the presence of 10% or 1% serum, and harvested every day for up to 5 d. After harvesting, the cells were stained with Trypan blue, and the total number of live cells as determined by Trypan blue dye exclusion were counted using a hemocytometer (Y axis) and plotted against the number of days (X axis).

Immunohistochemistry

Immunohistochemistry was performed as previously described (Jung et al., 2004). Briefly, slides containing colon cancer tissues were deparaffinized in xylene and rehydrated in graded alcohols. Slides were immersed in sodium citrate buffer (pH 6.0), and heated in a microwave 4 times, 4 min each, for antigen retrieval. Slides were then processed using a DAKO® Signal Catalyzed Amplification (CSA) System (DAKO Corporation, Carpinteria, CA). Endogenous peroxidase activity was blocked by incubation with H_2O_2. Ten percent goat serum was added for 15 min to block nonspecific protein binding. Slides were then incubated overnight with pc GIV-CTAb (6 µg/ml) and then rinsed with PBS. Biotinylated anti-rabbit IgG was added for 15 min followed by incubation with peroxidase-labeled streptavidin for 15 min at room temperature. Sections were washed with PBS, incubated with 3,3-diaminobenzidine (DAB) and H_2O_2 for 1 min, lightly counterstained with hematoxylin, dehydrated in graded alcohols, cleared in xylene, and coverslipped. Staining was scored as negative or positive by three independent observers blinded to patient outcome and stage.

Immunoblotting

Proteins samples were separated by 10% SDS-PAGE and transferred to PVDF membranes (Millipore, Billerica, MA). Membranes were blocked with PBS supplemented with 5% nonfat milk, then incubated sequentially with primary and secondary antibodies. Infrared imaging with two-color detection and quantification of Western blots was performed according to the manufacturer's protocols using an Odyssey imaging system (Li-Cor Biosciences, Lincoln, NE). When anti-phosphoprotein antibodies (anti-pAkt, anti-pSrc, anti-pSTAT, anti-pPLCγ1, anti-phosphotyrosine EGFR) were used, nonfat milk was replaced by BSA.

BIBLIOGRAPHY FOR SUPPLEMENTARY ONLINE MATERIALS:

Chmielowiec, J., Borowiak, M., Morkel, M., Stradal, T., Munz, B., Werner, S., Wehland, J., Birchmeier, C., and Birchmeier, W. (2007). c-Met is essential for wound healing in the skin. J Cell Biol *177*, 151-162.

Enomoto, A., Murakami, H., Asai, N., Morone, N., Watanabe, T., Kawai, K., Murakumo, Y., Usukura, J., Kaibuchi, K., and Takahashi, M. (2005). Akt/PKB regulates actin organization and cell motility via Girdin/APE. Developmental cell *9*, 389-402.

Garcia-Marcos, M., Ghosh, P., and Farquhar, M.G. (2009). GIV is a nonreceptor GEF for G alpha i with a unique motif that regulates Akt signaling. Proceedings of the National Academy of Sciences of the United States of America *106(9)*, 3178-3183.

Garcia-Marcos, M., Ghosh, P., Farquhar, MG (2008). GIV is a non-receptor GEF for Gαi with a unique motif that regulates Akt signaling Proceedings of the National Academy of Sciences (*PNAS*), Accepted, In press, Jan 2009. .

Garcia-Marcos, M., Ghosh, P., Farquhar, MG (2009). GIV is a non-receptor GEF for Gαi with a unique motif that regulates Akt signaling Proceedings of the National Academy of Sciences (*PNAS*).

Ghosh, P., Garcia-Marcos, M., Bornheimer, S.J., and Farquhar, M.G. (2008). Activation of Galphai3 triggers cell migration via regulation of GIV. J Cell Biol *182*, 381-393.

Gill, G.N., Kawamoto, T., Cochet, C., Le, A., Sato, J.D., Masui, H., McLeod, C., and Mendelsohn, J. (1984). Monoclonal anti-epidermal growth factor receptor antibodies which are inhibitors of epidermal growth factor binding and antagonists of epidermal growth factor binding and antagonists of epidermal growth factor-stimulated tyrosine protein kinase activity. J Biol Chem *259*, 7755-7760.

Hans, F., and Dimitrov, S. (2001). Histone H3 phosphorylation and cell division. Oncogene *20*, 3021-3027.

Jung, B., Doctolero, R.T., Tajima, A., Nguyen, A.K., Keku, T., Sandler, R.S., and Carethers, J.M. (2004). Loss of activin receptor type 2 protein expression in microsatellite unstable colon cancers. Gastroenterology *126*, 654-659.

Kodani, A., and Sutterlin, C. (2008). The Golgi protein GM130 regulates centrosome morphology and function. Molecular biology of the cell *19*, 745-753.

Le-Niculescu, H., Niesman, I., Fischer, T., DeVries, L., and Farquhar, M.G. (2005). Identification and characterization of GIV, a novel Galpha i/s-interacting protein found on COPI, endoplasmic reticulum-Golgi transport vesicles. J Biol Chem *280*, 22012-22020.

Noma, T., Lemaire, A., Naga Prasad, S.V., Barki-Harrington, L., Tilley, D.G., Chen, J., Le Corvoisier, P., Violin, J.D., Wei, H., Lefkowitz, R.J., and Rockman, H.A. (2007). Beta-arrestin-mediated beta1-adrenergic receptor transactivation of the EGFR confers cardioprotection. The Journal of clinical investigation *117*, 2445-2458.

Qiao, M., Iglehart, J.D., and Pardee, A.B. (2007). Metastatic potential of 21T human breast cancer cells depends on Akt/protein kinase B activation. Cancer research *67*, 5293-5299.

Razi, M., and Futter, C.E. (2006). Distinct roles for Tsg101 and Hrs in multivesicular body formation and inward vesiculation. Molecular biology of the cell *17*, 3469-3483.

Simpson, F., Martin, S., Evans, T.M., Kerr, M., James, D.E., Parton, R.G., Teasdale, R.D., and Wicking, C. (2005). A novel hook-related protein family and the characterization of hook-related protein 1. Traffic *6*, 442-458.

Shapiro, M.B., and Senapathy, P. (1987). RNA splice junctions of different classes of eukaryotes: sequence statistics and functional implications in gene expression. Nucleic Acids Res *15*, 7155-7174.

SUPPLEMENTARY FIGURE LEGENDS:

Fig S1: Characterization of HeLa epithelial cell lines used in the current work.
A. Comparison of steady-state levels of proteins expressed GIV-wt and GIV-FA cells. Equal aliquots of lysates (~40 µg protein) from HeLa cell lines stably expressing either wild-type GIV (GIV-wt) or a dominant negative, GEF-deficient F1685A GIV mutant (GIV-FA), and control (untransfected) cells were analyzed for GIV, total EGFR, Gαi3, actin and total (tAkt) and phosphorylated Akt (pAkt) by immunoblotting (IB). Levels of GIV are ~3 fold higher in GIV-wt and GIV-FA cells compared to untransfected controls, whereas levels of EGFR and Gαi3 are equal among the 3 cell lines at steady-state. As demonstrated previously (Garcia-Marcos, 2008), GIV-wt, but not GIV-FA cells display enhanced Akt activity vs. untransfected controls.
B. Confirmation of efficient depletion of endogenous GIV by siRNA. Equal aliquots of lysates (~40 µg protein) from GIV-wt, GIV-FA or contol HeLa cells were treated with GIV or scramble (scr) siRNA, harvested after 48 h and analyzed for GIV, Gαi3 and tubulin by immunoblotting (IB). GIV depletion was estimated to be >90-95% by Odyssey Infrared Imaging.
C. GIV-wt cells preferentially migrate while GIV-FA cells preferentially proliferate even without depletion of endogenous GIV. Confluent monolayers of HeLa cells stably overexpressing either wild-type GIV (GIV-wt) or GEF-deficient GIV (GIV-FA) were scratch-wounded, treated with 0.1 nM EGF, and the edge of the wound was monitored by live-cell imaging as in Figure 1A, except that endogenous GIV was not depleted. The total number of cells along the edge of the wound that underwent either polarized migration into the wound (upper graph) or mitosis (lower graph) in response to EGF within 8 and 16 h were quantified and expressed as the % of total cells analyzed. Results are shown as mean +/- S.E.M. (n=3).

Fig S2: A, B. The mitotic index is low in GIV-wt and high in GIV-FA cells. A. Lysates of GIV-wt and GIV-FA cells were analyzed for Phospho-Histone H3 (pH3, Ser 28) and total H3 by immunoblotting (IB) before and after scratch-wounding. At 2 h after scratch-wounding, the pH3:H3 ratio is reduced by 80% in GIV-wt cells and 50% in controls, but remains virtually unchanged in GIV-FA cells. **B.** Left panel: Images obtained from the edge of the wound (demarcated by a white line). Confluent monolayers of GIV-wt, GIV-FA and control HeLa cells were stimulated to migrate by scratch-wounding, fixed at 8 h and costained for phospho-Histone H3 (pH3) and DAPI. Right panel: Bar graphs comparing the mitotic index 8 h after scratch-wounding, as determined by the number of cells at the edge of the wound displaying intense pH3 (red) signals associated with condensed chromatin by immunofluorescence (left panel, a-c), and expressed as the percent of total cells counted (DAPI-positive, blue). Among the GIV-FA cells counted at the wound edge, ~33-35% stain positive for pH3, which is higher than control HeLa cells (~25-27%), whereas only ~13% of GIV-wt cells stain for pH3. These results indicate that upon scratch-wounding, GIV-wt cells halt mitosis (low mitotic index), whereas GIV-FA cells continue to enter mitosis (high mitotic index). Results are shown as mean +/- S.E.M (n=3).

S3: EGFR phosphorylation and downstream signaling in control, GIV-WT, and GIV-FA cells after depletion of endogenous GIV.
A. GIV-wt cells enhance motogenic signals and GIV-FA cells enhance mitogenic signals, whereas depletion of endogenous GIV from controls suppresses both. Control HeLa (untransfected) and HeLa cells stably expressing siRNA-resistant GIV-wt or GIV-FA were treated with GIV siRNA to deplete endogenous GIV, starved overnight in the presence of 0.2% FBS, stimulated with 50 nM EGF for various times, and whole cell lysates were analyzed for total (t) and phospho (p) PLCγ1, pSTAT5, c-Src, Akt, ERK 1/2, and tubulin by immunoblotting (IB). Effective depletion (>85-90%) of endogenous GIV was achieved, whereas the levels of Gαi3 were similar. Signaling profiles of GIV-wt and GIV-FA cells are the same as those in Figure 1C (performed without depletion of endogenous GIV) in that upon ligand stimulation, pAkt and pPLCγ1 levels are higher in GIV-wt cells at 5 min and 15 min, respectively. In GIV-FA cells, levels of pSTAT5b and pERK1/2 are increased at 5 min and are sustained at 15 min. The levels of inhibitory phosphorylation of c-Src at Y527 were high in GIV-wt and low in GIV-FA cells, indicating that Src activity

is suppressed in the former and enhanced in the latter. In contrast to cells expressing GIV-wt or GIV-FA, depletion of endogenous GIV from control HeLa cells abrogated signaling of all pathways studied—i.e., PLCγ1, pSTAT5, c-Src, Akt, and ERK 1/2. Results from one representative experiment are displayed (n= 3).

B. GIV-wt, GIV-FA, and GIV-depleted cells have distinct profiles of EGFR phosphorylation and receptor degradation. Control HeLa (untransfected) and HeLa cells stably expressing siRNA-resistant GIV-wt or GIV-FA were treated with GIV siRNA for 36 h, serum starved for 12 h, stimulated with 50 nM EGF as in S3A, and whole cell lysates were then analyzed for tEGFR and pEGFR using phospho-Tyr-site specific antibodies to Y845 and Y992 by immunoblotting (IB) as in 2B. Findings are identical to those displayed in Figure 2B and 3C (performed without depletion of endogenous GIV) in that, upon ligand stimulation increased receptor autophosphorylation at Y992 occurs in GIV-wt cells, whereas sustained phosphorylation at Y845 is seen in GIV-FA cells, and EGFR degradation is delayed (compare tEGFR) in GIV-FA cells vs. GIV-wt and GIV-depleted HeLa controls. Results from one representative experiment are shown (n = 2).

Fig S4: Interaction of endogenous GIV and EGFR in Cos7 cells.

A. Serum starved Cos7 cells were stimulated with 50 nM EGF for 5 min, lysed and endogenous EGFR was immunoprecipitated from equal amounts of lysates (INPUT; left panel) with preimmune mAb or anti-EGFR #225 mAb, as in Figure 4A. Right Panel: Immune complexes were analyzed for tEGFR and p-EGFR (Y845), Gαi3 and GIV by immunoblotting (IB). Results were identical to those obtained with HeLa cells, shown in 4A.

B. Endogenous Gαi3 and EGFR do not show significant colocalization at the cell periphery in the starved state (before ligand stimulation). Serum starved HeLa cells were stained for Gαi3 (**a**, red), total EGFR (**b**, green; Anti-EGFR #225 mAb), and the nucleus/DAPI (blue), and analyzed by confocal microscopy. Merged image (**c**) shows EGFR, but not Gαi3 staining along the cell periphery, presumably at the PM (arrowheads). Bar = 10 µM.

Fig S5: Analysis of GIV expression by RTPCR.

A. Domain organization of GIV and the domain-specific oligonucleotide primer pairs used for detection of GIV. The N-terminal Hook domain (purple) interacts with microtubules, the coiled-coil domain (green) mediates homodimerization, the Gα-binding domain (GBD, yellow) interacts with Gα subunits (Gi 1,2,3) (Le-Niculescu et al., 2005) and the extreme C-terminus (pink) interacts with Akt kinase and actin and harbors the critical GEF motif (black) through which GIV binds and activates Gi. The amino acids forming the boundaries of GIV's various domains are indicated. Regions within the coding sequence that were used to design various domain-specific oligonucleotide primer pairs are listed as 1 through 3. As illustrated, the primers span the central and 3' coding frame covering the C-terminal half of the protein: the coiled coil domain (CC), the Gα-binding domain (GBD) and the extreme C-terminus (CT) of hGIV. The corresponding coding exon numbers are indicated. Fw, forward; Rev, reverse.

Table 1: Expected sizes (bp) of PCR products obtained during RT-PCT using the indicated combinations of forward and reverse oligonucleotide primer pairs. cc, Coiled-coil; GBD, Gα-binding domain; ct, Carboxyl terminus; Fwd, forward; Rev, reverse.

B, C: A full length GIV transcript is expressed in human breast and colon epithelia. The GIV transcript in normal colon **(B)** and breast **(C)** epithelia was analyzed by RT-PCR using primers (illustrated in **Figure S5A**) to amplify consecutive, overlapping sequences encompassing the central and 3' coding region of the GIV gene. Arrowheads denote the products of expected size obtained using the various primer combinations tabulated in **S5A**. Sequence analysis confirmed that a full length normal transcript (Reference Sequence, NM_018084) is present in normal adult breast and colon epithelia.

Fig S6: Alternative splicing by intron retention effectively downregulates mature GIV transcript in poorly metastatic cancer cells.

A. Validation of detected intron retention using RT-minus (RT-) control. RNA isolated from the Ls174T and HT-29 cancer cell lines were subjected to RT-plus and RT-minus assays using exon #19 forward and #20 reverse primer pairs (see **Methods**). As shown in Figure 6A, in the RT-plus conditions a large amount of an unexpected ~1250-1300 bp long PCR product was amplified in HT-29p cells (right panel) along with a small amount of the PCR product of expected size (~250-300 bp, lower bands). In Ls174T cells, the expected ~250-300 bp PCR product was virtually replaced by the ~1250-1300 bp product. No amplified products are seen under RT-minus conditions, indicating that the isolated RNA was free of genomic DNA contaminants. The doublets observed in a 2% agarose gel represent a previously identified (Simpson et al., 2005) isoform in all tissues.
B. The abundance of GIV mRNA in poorly metastatic cells is inversely proportional to the % intron retention (Figure 6B). RNA isolated from cancer cells of variable metastatic potential (N, normal; H, high; L, low) was analyzed for abundance of the translated mature full length GIV RNA using different oligonucleotide primer pairs spanning the C-terminal region of the gene that contains G-binding and GEF domains (illustrated in C). The amount of GIV transcript obtained using each primer combination was consistently higher in highly motile/invasive MDA-MB231 and DLD1 cells compared to their normal breast and colon epithelia counterparts. Levels of full length GIV transcript in poorly motile/invasive MCF7, HT-29p and Ls174T cells were consistently lower than in normal cells, and inversely correlated with their percent intron retention (**Figure 6B**). In HT29p and Ls174T cells, where % intron retention is high, GIV mRNA is virtually undetectable.
C. Schematic illustration of the functional domains of GIV and the corresponding coding exons. Each blue box represents coding exons that are numbered 5' to 3'. Exons encoding specific functional domains are indicated using brackets. The GEF motif is located within exon #29.
D. The alternative splice site flanking intron 19 is weak. Yellow numbered boxes represent coding exonic sequences. Intronic sequence with highlighted 5' (donor) and 3' splice sites (branch point, red; poly (Y) track, green; and acceptor) and corresponding optimal mammalian splicing site consensus is illustrated. Optimum mammalian 5' and 3' splice site sequences are listed. In keeping with the GU-AG rule for splicing (Shapiro and Senapathy, 1987) the 5' and 3' boundaries of the 19th intron has a 5' donor splice site beginning with GU dinucleotide and a 3' acceptor site ending with an AG dinucleotide. When analyzed for its strengths as a splice site (see Methods), based on the sequence of the nucleotides flanking the 5' and 3' sites this intron is rated as a 'weak' site lacking homology to the consensus mammalian splice signals.

Figure S7: GIV is only expressed in modest amounts in the normal colonic epithelium and is highly expressed in stromal tissue. Paraffin embedded normal human colonic tissue was analyzed for full length GIV by immunohistochemistry using GIV-CTAb. **a.** No staining is seen in the negative control (Neg Ctrl) without primary antibody. **c.d.** Strong staining (brown) of stromal connective tissue and blood vessels (S) is seen with GIV-CT antibody as demonstrated previously (Kitamura et al., 2007; Jiang et al., 2007). Mild to moderate staining is also observed in epithelia lining the normal colonic crypts (**C**, arrowheads)**.**

SUPPLEMENTAL MOVIES

Movies 1, 2: HeLa cells expressing GIVwt are highly motile (Movie 1) whereas those expressing GEF-deficient GIVF1685A mutant show reduced motility and increased mitosis (Movie 2). Hela cells stably expressing siRNA-resistant GIV-wt or GIV-F1685A were treated with siRNA to deplete endogenous GIV. Cells were monitored simultaneously for motility and mitosis for 12 h at the edge of a freshly made wound (marked by a solid line) by live cell imaging. A mitotic event was defined as one where two daughter cells became clearly visible (arrows). Persistent directional motility, as determined by efficient cell-spreading, polarization and formation of a discernable leading edge, detachment from neighboring cells, and migration into the wound area, is frequently displayed by GIV-wt, but less so by GIV-FA cells. By contrast, mitosis is increased among GIV-FA cells compared to GIV-wt cells. Efficient closure of the

wound area by GIV-wt cells is attributable mostly to cell migration (movie 1), whereas a modest closure by GIV-FA cells is attributable mostly to enhanced cellular proliferation and cells at the edge being pushed from behind (movie 2).

Movies 3, 4. HeLa cells expressing the active Gαi3 Q204L mutant are highly motile (Movie 3) whereas those expressing the inactive Gαi3 G203A mutant show reduced motility and increased mitosis (Movie 4). Constitutively active (GTPase deficient) Gi3-Q204L-YFP (movie 3) or inactive Gi3-G203A-YFP (movie 4) were expressed in HeLa cells and monitored for 8 h for motility and mitosis at the edge of a freshly made wound by live cell imaging. Both of the Gαi3-YFP variants behave similarly to wt Gi3-YFP (Ghosh et al., 2008) in that they localize to the Golgi and pseudopods at the leading edge. Persistent directional motility, as determined by efficient migration into the wound area, is frequently displayed by cells expressing Gαi3QL, but not Gαi3GA. By contrast, mitosis is infrequent among cells expressing Gi3QL, but is increased among those expressing Gi3GA. The Gi3-YFP-transfected and untransfected cells were simultaneously monitored through the YFP and DIC channels, respectively.

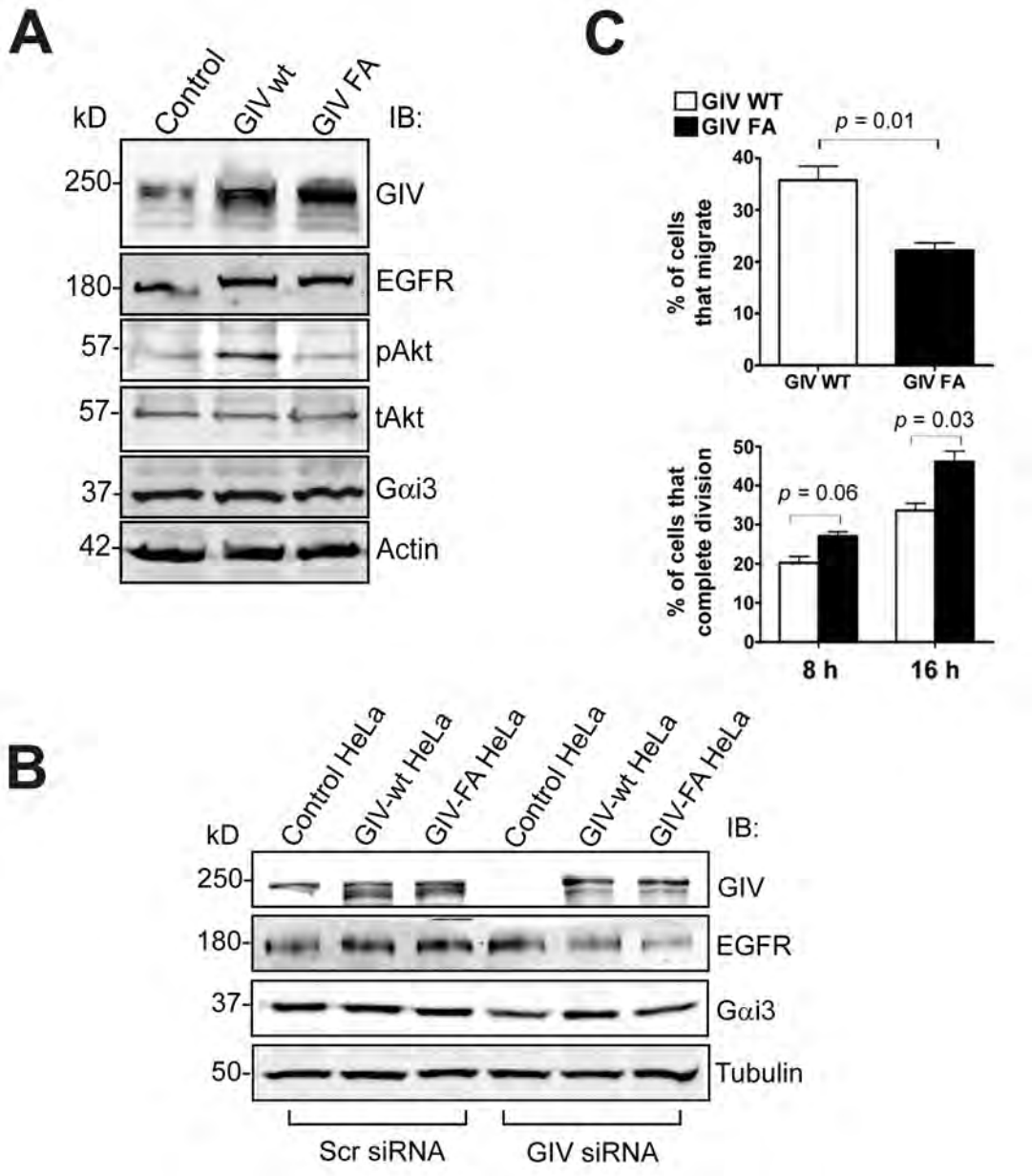
A
kD
Control
GIV wt
GIV FA
IB:
250
GIV
180
EGFR
57
pAkt
57
tAkt
37
Gαi3
42
Actin
C
GIV WT
GIV FA
p = 0.01
% of cells that migrate
40
30
20
10
0
GIV WT
GIV FA
p = 0.03
p = 0.06
% of cells that complete division
50
40
30
20
10
0
8 h
16 h
B
kD
Control HeLa
GIV-wt HeLa
GIV-FA HeLa
Control HeLa
GIV-wt HeLa
GIV-FA HeLa
IB:
250
GIV
180
EGFR
37
Gαi3
50
Tubulin
Scr siRNA
GIV siRNA

Figure S1

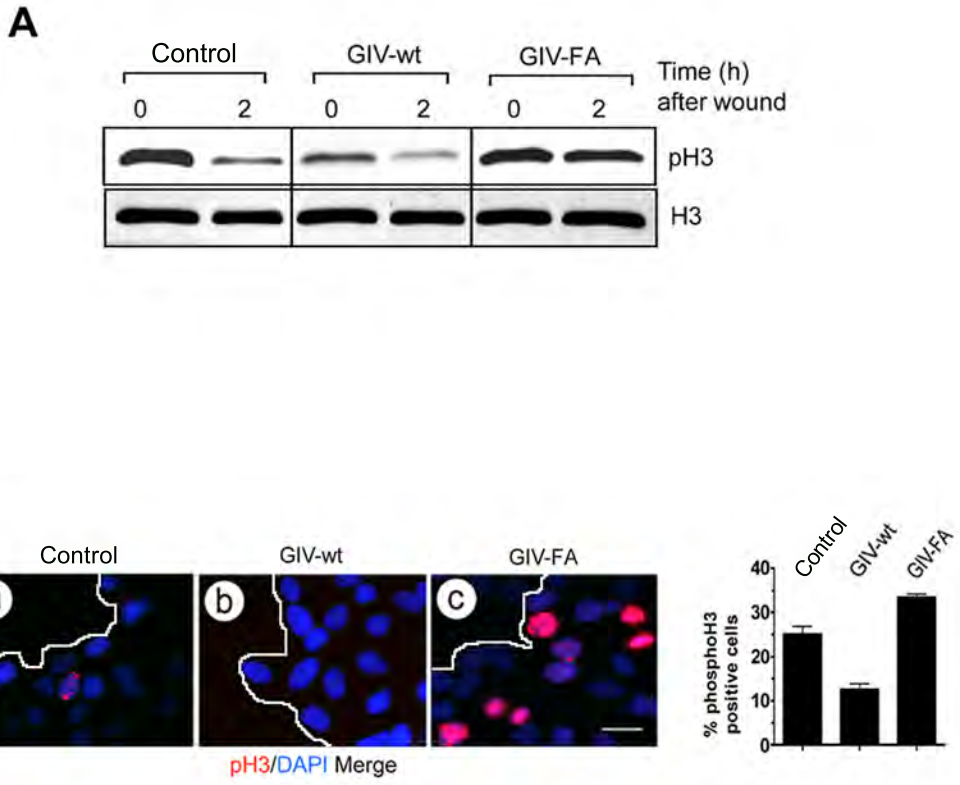
A
Control
GIV-wt
GIV-FA
Time (h)
after wound
0
2
0
2
0
2
pH3
H3
B
Control
GIV-wt
GIV-FA
a
b
c
pH3/DAPI Merge
% phosphoH3
positive cells
40
30
20
10
0
Control
GIV-wt
GIV-FA

Figure S2

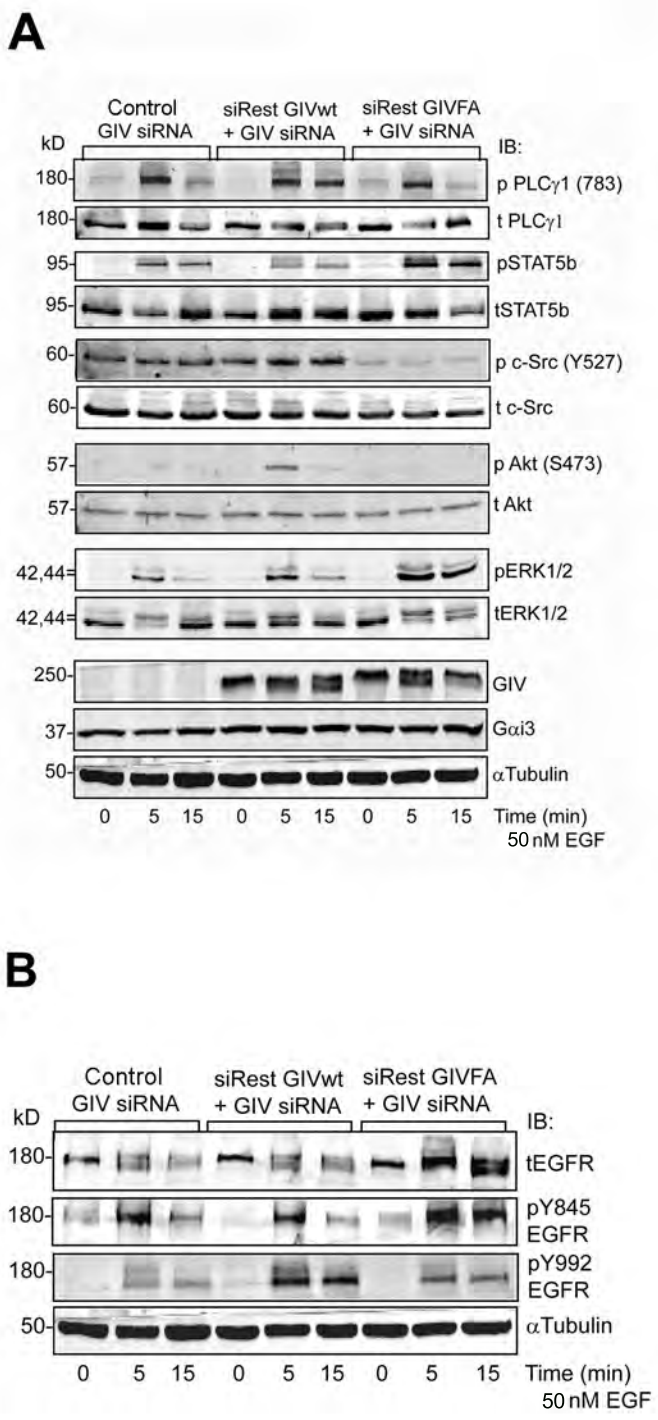
A
Control
GIV siRNA
siRest GIVwt
+ GIV siRNA
siRest GIVFA
+ GIV siRNA
kD
IB:
180-
p PLCγ1 (783)
180-
t PLCγ1
95-
pSTAT5b
95-
tSTAT5b
60-
p c-Src (Y527)
60-
t c-Src
57-
p Akt (S473)
57-
t Akt
42,44=
pERK1/2
42,44=
tERK1/2
250-
GIV
37-
Gαi3
50-
αTubulin
0 5 15 0 5 15 0 5 15
Time (min)
50 nM EGF
B
Control
GIV siRNA
siRest GIVwt
+ GIV siRNA
siRest GIVFA
+ GIV siRNA
kD
IB:
180-
tEGFR
180-
pY845
EGFR
180-
pY992
EGFR
50-
αTubulin
0 5 15 0 5 15 0 5 15
Time (min)
50 nM EGF

Figure S 3

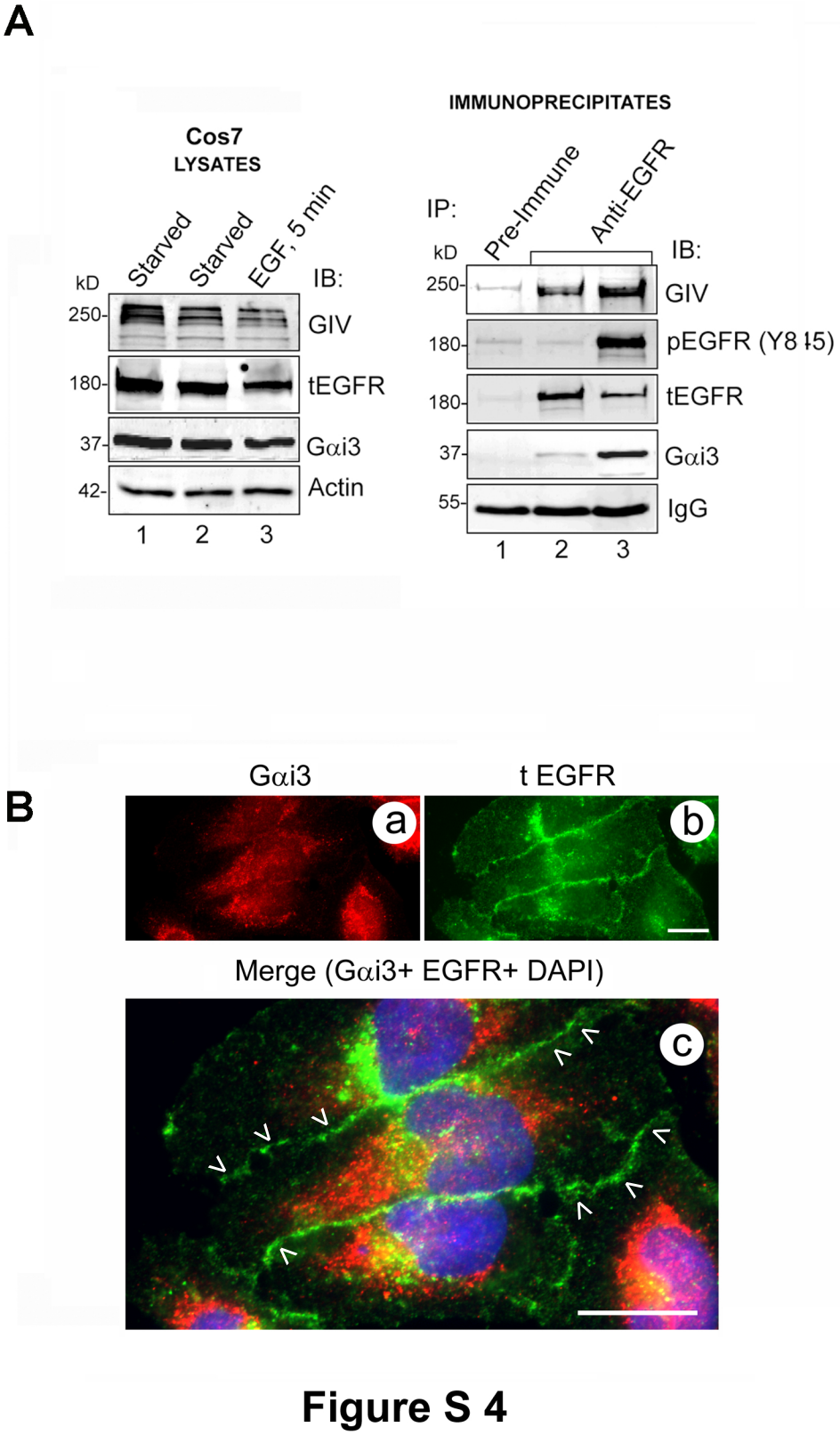
A
Cos7
LYSATES
Starved
Starved
EGF, 5 min
kD
IB:
250-
GIV
180-
tEGFR
37-
Gαi3
42-
Actin
1 2 3
IMMUNOPRECIPITATES
IP:
Pre-Immune
Anti-EGFR
kD
IB:
250-
GIV
180-
pEGFR (Y845)
180-
tEGFR
37-
Gαi3
55-
IgG
1 2 3
B
Gαi3
t EGFR
a
b
Merge (Gαi3+ EGFR+ DAPI)
c

Figure S 4

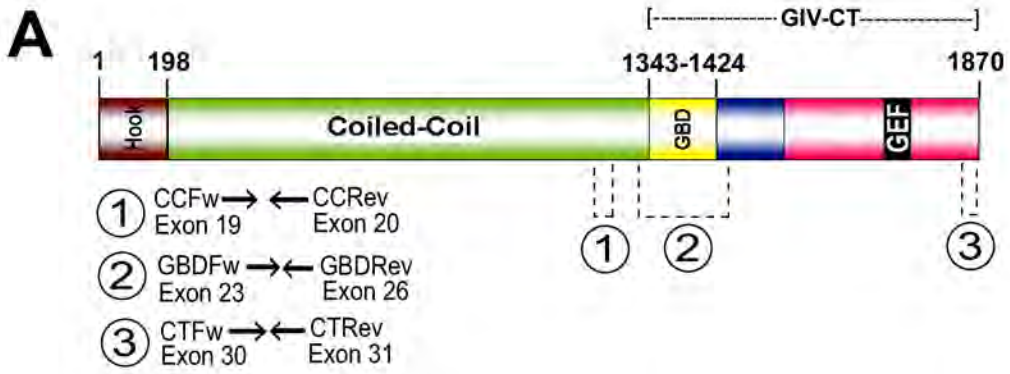

Table 1

	hGIV cc Rev	hGIV ct Rev	hGIV GBD Rev
hGIV cc Fwd	246	2230	1274
hGIV ct Fwd		204	
hGIV GBD Fwd		1786	830

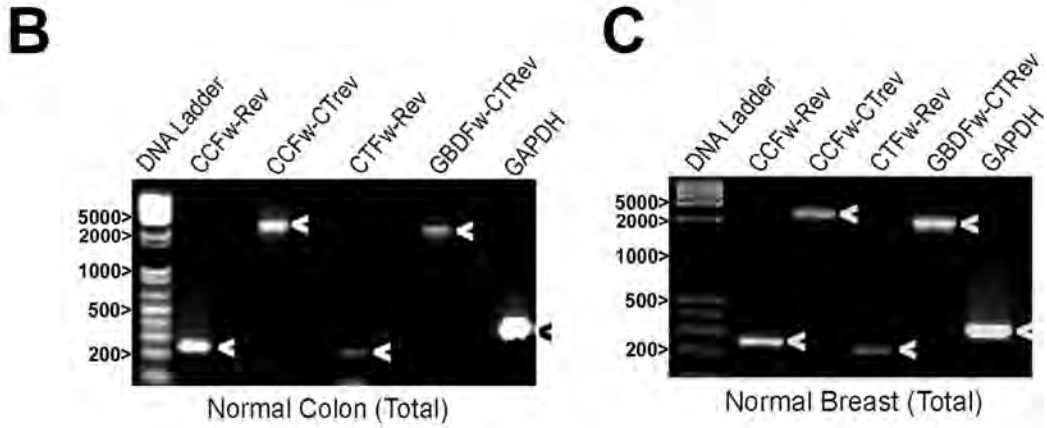

Figure S5

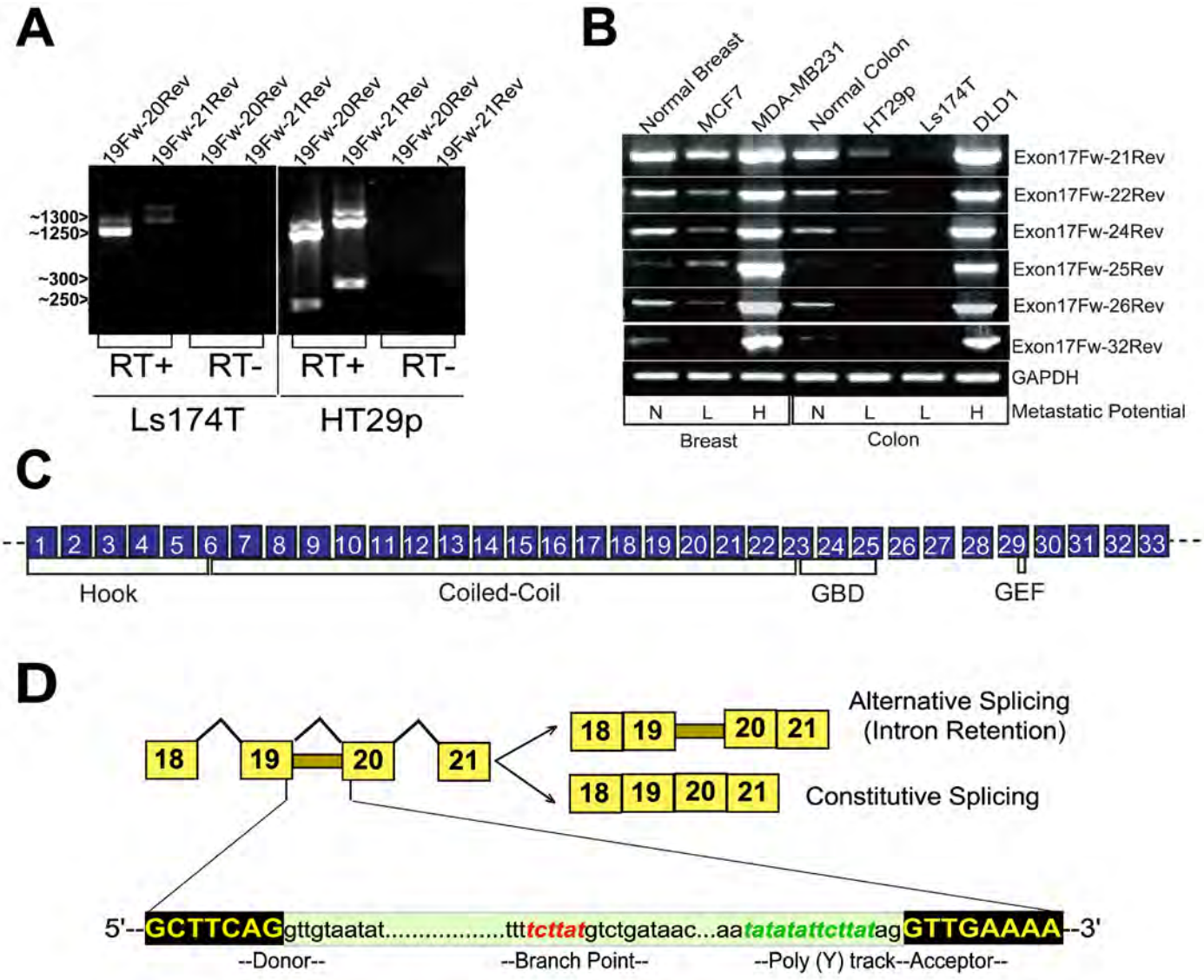
A
19Fw-20Rev
19Fw-21Rev
~1300>
~1250>
~300>
~250>
RT+
RT-
Ls174T
HT29p
B
Normal Breast
MCF7
MDA-MB231
Normal Colon
HT29p
Ls174T
DLD1
Exon17Fw-21Rev
Exon17Fw-22Rev
Exon17Fw-24Rev
Exon17Fw-25Rev
Exon17Fw-26Rev
Exon17Fw-32Rev
GAPDH
N L H N L L H
Metastatic Potential
Breast
Colon
C
Hook
Coiled-Coil
GBD
GEF
D
Alternative Splicing
(Intron Retention)
Constitutive Splicing
5'--GCTTCAGgttgtaatat.....tttTCTTATgtctgataac...aaTATATATTCTTATagGTTGAAAA--3'
--Donor--
--Branch Point--
--Poly (Y) track--Acceptor--
Optimal 5' and 3' splice sites: 5'---AGgtRagt.....(Y)ncagGT---3'
Optimal Branch point consensus: TNCTRAT/C
Optimal p(Y) track: five uninterrupted Ts
R= purine (A/G)
Y= pyrimidine (T/C)

Figure S6

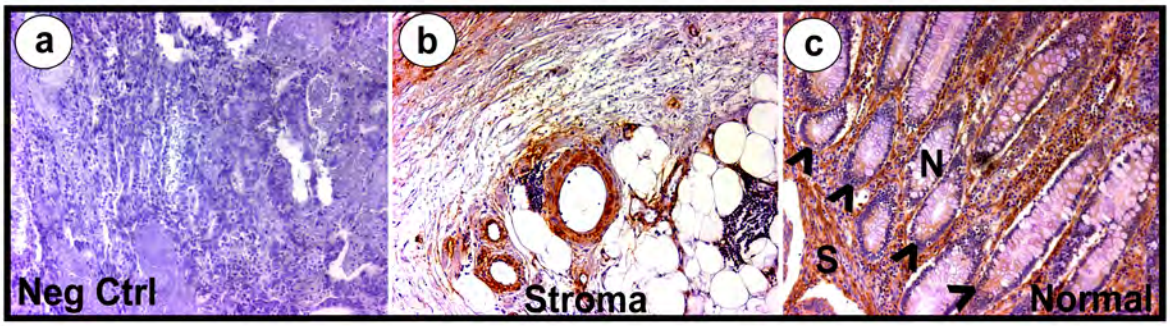

Figure S7